European Journal of Pharmaceutical Sciences 138 (2019) 104990

Contents lists available at ScienceDirect

European Journal of Pharmaceutical Sciences

journal homepage: www.elsevier.com/locate/ejps

Pore change during degradation of octreotide acetate-loaded PLGA microspheres: The effect of polymer blends

Tengteng Wang[a], Peng Xue[b], Aiping Wang[a], Miaomiao Yin[a], Junping Han[a], Shengnan Tang[a], Rongcai Liang[a,*]

[a] School of Pharmacy, Collaborative Innovation Center of Advanced Drug Delivery System and Biotech Drugs in Universities of Shandong, Key Laboratory of Molecular Pharmacology and Drug Evaluation (Yantai University), Ministry of Education, Yantai University, Yantai, Shandong Province, People's Republic of China
[b] State Key Laboratory of Long-Acting and Targeting Drug Delivery System, Shandong Luye Pharmaceutical Co., Ltd., Yantai, Shandong Province, People's Republic of China

ARTICLE INFO

Keywords:
PLGA blends
Microspheres
Swelling
Pores
Release profile

ABSTRACT

The purpose of this study was to solve the plateau phase (the stage in which the drug in the microsphere undergoes a slow release or almost no release after initial release) problem by understanding the effect of polymer blends on the internal pore changes of the microspheres. This study used PLGA 5050 4H (F-1), PLGA 5050 1A: PLGA 5050 4H = 3:7 (F-2) and PLGA 7525 1A: PLGA 5050 4H = 3:7 (F-3) as a carrier, respectively. Microspheres (MS) were obtained by O/W emulsion solvent evaporation technique and characterized by scanning electron microscopy (SEM), particle size, drug loading, fluorescence characteristics, and in vitro and in vivo release. Accelerated tests in vitro showed that the size and number of core pores significantly affected drug release in the first and second phases. After intramuscular administration, F-2 and F-3 showed effective blood concentration levels and their bioavailability was higher than that of the RLD (Sandostatin Lar). In general, our data indicate that pore formation is unevenly distributed throughout PLGA MS prepared using polymer blends, and the use of polymer blends is instructive for the development of sustained smooth release microspheres. Therefore, the octreotide MS described in this study has a good clinical application potential for the treatment of acromegaly.

1. Introduction

Somatostatin (SST), a peptide hormone, has been found to be an inhibitor of growth hormone release, which inhibits the regulation of various physiological functions, such as pituitary, pancreatic and gastrointestinal hormone secretion (Orlewska et al., 2018). It exerts a biological effect by interacting with a specific somatostatin receptor expressed on the target tissue (Aziz et al., 2018). Due to the extremely short half-life of SST in the body, its clinical application is hindered. Therefore, people are committed to the research and synthesis of somatostatin analogue (SSTA). Compared with natural SST, SSTA has the advantages of long plasma half-life, long-lasting effect, convenient use, and relatively single action (Orlewska et al., 2018). At present, the common standard for the clinical treatment of acromegaly and functional tumors of the gastrointestinal pancreatic endocrine system is SSTA (Tiberg et al., 2015). Somatostatin and its analogs include common somatostatin, lanreotide, octreotide, pareptide and the like (Aziz et al., 2018). Because of its good curative effect in the treatment of esophageal variceal bleeding, acute pancreatitis, and other digestive systems critical illness, it is “loved” by digestive physicians. Among them, octreotide acetate microspheres (MS) are effective dosage forms for long-acting effects of drugs. However, after the commercially available octreotide acetate MS was injected, the concentration of the drug quickly reached the first peak within 1 h after administration, most patients in the next 7 days maintained octreotide acetate below the therapeutic level (Casnici et al., 2018). In addition, patients with gastrointestinal pancreatic endocrine tumors should continue subcutaneous injection of Sandostatin for at least two weeks after the administration of octreotide acetate MS to maintain the efficacy of drug treatment (Sun et al., 2017). Therefore, it is extremely urgent to solve the problem of the octreotide acetate MS plateau phase (the stage in which the drug in the microsphere undergoes a slow release or almost no release after initial release).

PLGA MS is the best choice for delivering therapeutic proteins and peptides in a sustained release behavior. There are commercial long-acting release (LAR®) drug formulations of MS on the market (e.g.,

* Corresponding author at: School of Pharmacy, Yantai University, No 30 Qingquan Road, Yantai, 264005, Shandong Province, People's Republic of China.
E-mail address: liangrongcai@luye.com (R. Liang).

https://doi.org/10.1016/j.ejps.2019.104990
Received 14 May 2019; Received in revised form 26 June 2019; Accepted 7 July 2019
Available online 11 July 2019
0928-0987/

Lupron Depot®, Zoladex®, and Enantone®) (Chingle et al., 2017; Liu et al., 2017; Ohlmann and Gross-Langenhoff, 2018). Currently, the release of drugs from PLGA MS has been shown to be controlled by the following factors: i) drug dissolution, ii) PLGA degradation/erosion and iii) PLGA swelling (Fredenberg et al., 2011). The release profile of most PLGA MS is characterized by a burst release followed by a plateau phase and a rapid release of the drug. However, the potential mass transfer mechanisms in PLGA MS are not completely understood. The complexity of the mass transfer mechanism is the main cause of this phenomenon. According to the literature, the initial release and plateau phase are the main causes of fluctuations in drug concentration in the bloodstream, which may cause various adverse reactions (Hu et al., 2011). Many studies have reported that the nature of polymers is a major element influencing the rate of drug release in biodegradable polymer materials. Degradation of high molecular weight (Mw) PLGA results in a longer plateau phase than low molecular weight (Mw) PLGA because of its higher hydrophobicity results in a slower rate of solution penetration into the polymer (Huang et al., 2015). The degradation rate of high Mw PLGA is accelerated by the strong water absorption of low Mw PLGA and the increase of autocatalytic acidic products, mixing high Mw PLGA with low Mw PLGA is an interesting foreground (Wang and Gu, 2014).

In this study, we used octreotide acetate as a model drug to obtain MS for sustained release of octreotide and long-term therapy of acromegaly by using different polymer blends and improved preparation methods. On this basis, we investigated the mechanism of mixed high and low Mw PLGA affecting drug release by observing the changes in the internal structure of PLGA MS at different release stages, thereby providing new ideas for clinical treatment of patients with acromegaly.

2. Materials and methods

2.1. Materials

Octreotide acetate was selected from Shanghai Soho Yiming Pharma Company; RLD (Sandostatin Lar) were purchased through Novartis. The manufacturer of PLGA 7525 1A (MW 5000 Da), 5050 1A (MW 5000 Da), and 5050 4H (MW 51000 Da) is Lakeshore Biomaterials (Alabama, USA). Methanol (chromatographic grade) and dichloromethane (analytical grade) were selected from Tianjin Bodi Chemical Company; Polyvinyl alcohol (PVA, 80% hydrolyzed, Mw 9–10 kDa) was selected from MERCK. All other chemicals were of analytical or chromatographic grade.

Sprague Dawley rats (male; 180–220 g) were offered by Experimental Animal Company of Jinan Pengyue. Rats were housed in an environment of 22 ± 1 °C and provided with standard diet and water. All animal experiments were in accordance with the guidelines of the Ethical Committee on Animal Experimentation of Yantai University (Yantai, China) and were in compliance with the EU Directive 2010/63/EU and the National Institutes of Health Guide for the Care and Use of Laboratory Animals.

2.2. Preparation of microsphere

According to the composition given in Table 1, an O/W emulsion solvent evaporation technology was used to obtain a microsphere formulation loaded with octreotide acetate. The octreotide acetate and PLGA were exactly weighed and dispersed in 2 ml of methanol and 14 ml of dichloromethane, respectively. Then, the octreotide acetate solution was added to the PLGA dichloromethane and stirred to homogenize. The mixture was added to 1000 ml of 1% PVA solution by a peristaltic pump and then homogenized at 3000 rpm for 2.5 min. The resulting emulsion was mechanically stirred (300 rpm, 5 h) to solidify the microspheres and evaporate dichloromethane. Then, the resulting solution was passed through a sieve (5 μm) to collect the MS, which were rinsed with purified water for 3 to 5 times. Finally, it was transferred to a Petri dish, vacuumed for 24 h, lyophilized and passed through a sieve (150 μm) to mix the MS.

2.3. Particle size analysis

MS was suspended in 0.1% (w/w) Tween-20 solution and the size of particles was determined using the Mastersizer 2000 Particle Analyzer (Malvern, England). The samples of each group were measured in triplicate and the results were expressed as average values.

2.4. Drug loading and encapsulation efficiency

25 mg of octreotide acetate-containing PLGA MS were dissolved in 25 ml acetic acid. HPLC was used to measure the concentration of octreotide acetate in the supernatant after centrifugation. The formula for drug loading and encapsulation efficiency is as follows:

Drug loading (%)

= (The weight of drug in microspheres/The weight of microspheres) * 100

Encapsulation efficiency (%)

= (Encapsulated drug in microspheres/Total amount of drug in microspheres) * 100

2.5. Differential scanning calorimetry (DSC)

The octreotide acetate, PLGA, octreotide acetate-PLGA powder mixture, and the MS lyophilized powder were respectively placed in an aluminum pan as a test object; and the empty sample pan was taken as a reference. The analyte and the standard were placed in the DSC (DSC822^e, METTLER) at the same time, and the scanning temperature was set to 0–200 °C, and the heating rate was 10 °C/min.

2.6. Fluorescence spectrophotometer and laser scanning confocal microscope (LSCM)

The optimal emission and excitation wavelength of octreotide acetate was determined by a fluorescence spectrophotometer (LS-55, PerkinElmer).

LSCM (TCS SP8, Leica) was mainly used to study the distribution of octreotide acetate on the surface of MS. Place it on a glass slide, select the optimum wavelength and take a fluorescent image. The release behavior of the microspheres was initially determined based on the

Table 1
Composition and characteristics of microsphere formulations using polymer blends.

Formulation	octreotide(mg)	PLGA (mg) 5050 1A	PLGA (mg) 7525 1A	PLGA (mg) 5050 4H	Drug loading (%)	Encapsulation efficiency (%)	Particle size d (0.5) μm
F-1	330	–	–	3000	5.51	55.1	64.9
F-2	330	900	–	2100	4.87	48.7	59.5
F-3	330	–	900	2100	5.15	51.5	60.4

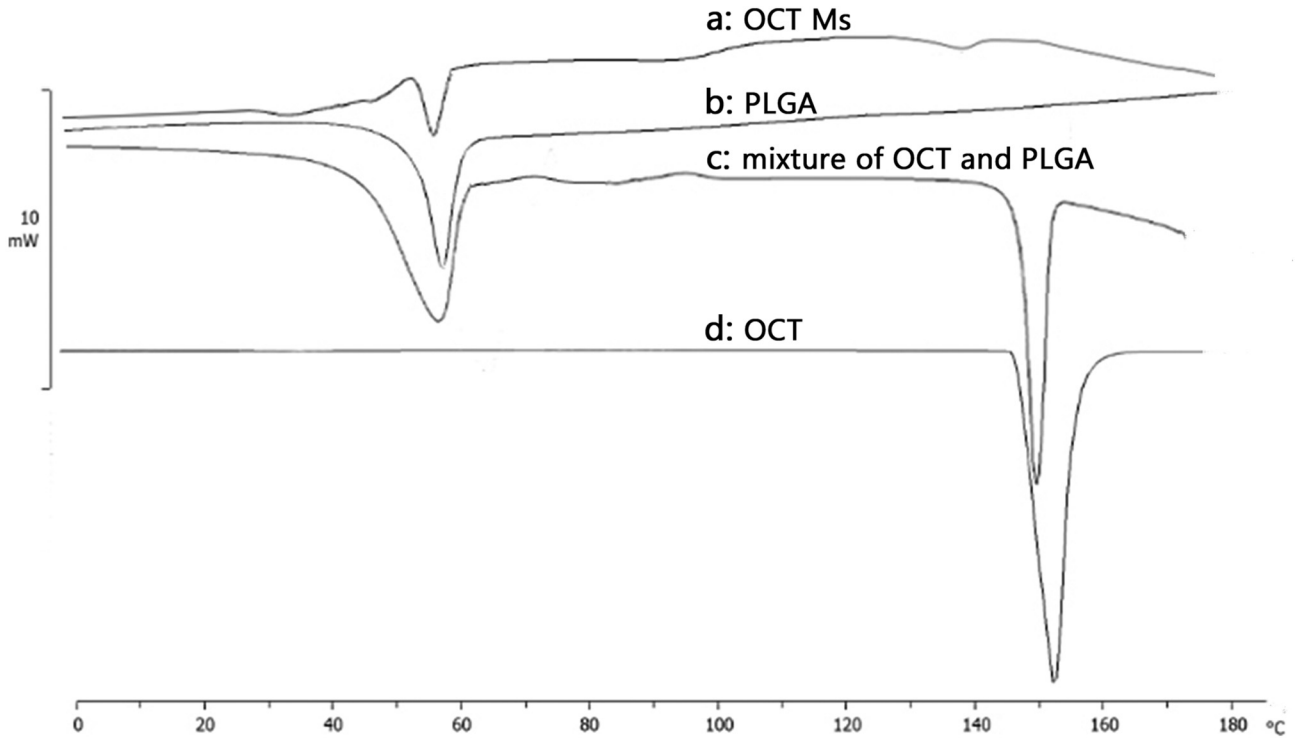

Fig. 1. DSC results of PLGA(b), octreotide (d), octreotide-PLGA powder mixture (c) and octreotide microspheres (a).

fluorescence intensity.

2.7. Accelerated in vitro release testing

The MS (≈30 mg) were distributed in 5 ml methanol-water (ratio 1:20) at 45 °C and shaken at 50 rpm in the constant temperature bath oscillator (HZS-HA, Harbin, China). The samples were analyzed at 0.15 h, 0.25 h, 0.5 h, 1 h, 3 h, 6 h, 12 h,1 d, 2 d, 3 d, 4 d, 5 d, 6 d, 7 d, 8 d, 9 d, 11 d, 13 d and 4 ml of methanol-water solution was added.

The analysis of octreotide acetate used a high-performance liquid chromatography system equipped with an XB-C18 column (5 μm, 4.6 mm × 250 mm, 300 A). The drug content was analyzed using a mobile phase of 0.5% phosphoric acid acetonitrile/0.5% phosphoric acid water (24/76, v/v), a flow rate of 1 ml/min, and a detection wavelength of 210 nm.

2.8. Morphology of microspheres

First, a suitable amount of the MS lyophilized powder was placed in a petri dish, cooled by adding an appropriate amount of liquid nitrogen, and then cut with a razor blade. Then, the sample was fixed on a flat plate with double-sided tape, subjected to surface gold spray treatment under vacuum, and the surface and cross-sectional morphology of the MS were looked by scanning electron microscope (SEM, EM-30PLUS, Coxem, Korea).

2.9. Pharmacokinetic study

SD rats were randomly divided into four groups of five rats each. Animals were all fasted for 12 h with access to water ad libitum prior to dosing. The RLD (Sandostatin Lar), F-1, F-2, and F-3 were injected intramuscularly at a single dose of 10 mg/kg. The blood octreotide acetate concentrations were analyzed at 0, 0.25, 0.5, 2 and 6 h, and 1, 2, 4, 7, 13, 16, 20, 25, 30, 35, 40, 45 and 50 d. The concentration of octreotide acetate in the plasma was measured by using ultra performance liquid chromatography-tandem mass spectrometry (UPLC–MS/MS, Waters Corp., Milford, MA).

2.10. Statistical analysis

All measurements in the experiment were mean ± SD. DAS 2.0 software was used to obtain pharmacokinetic parameters.

3. Results

3.1. Particle size, drug loading, and encapsulation efficiency

We then focused on three types of microparticles, prepared from polymers of different PLGA (5050 4H, a mixture of 5050 1A and 5050 4H, a mixture of 7525 1A and 5050 4H). The particle size, drug loading and encapsulation efficiency of the microparticles obtained with these polymers (F-1, F-2, and F-3, respectively) are presented in Table 1. It was easy to find differences in the particle sizes of these three formulations. In contrast, F-2 and F-3 have smaller particle sizes. It is conjectured that since the concentration of the polymer in the three formulations is the same, the reduction of intrinsic viscosity due to a decrease in polymer Mw leads to a reduction in the particle size of the MS (F. Y. Han et al., 2016a). In addition, the drug loading of F-1 was the highest, and the addition of low Mw PLGA may reduce the drug loading and encapsulation efficiency of the MS to some extent.

3.2. DSC

DSC analysis of octreotide acetate, PLGA, physical mixture of free octreotide acetate and PLGA, and PLGA-MS were shown in Fig. 1. The mixture of PLGA and octreotide acetate had a distinct endothermic peak around 57 °C and 150 °C, which was likely based on the fact that the polymer and the drug were only present in the physical mixture of the crystalline form of the drug. The melting point of octreotide acetate (~138–140 °C) in the MS was significantly lower than that of its pure form(~150–152 °C). This indicates that the crystallization characteristics of the drug were changed during the preparation of the MS. The

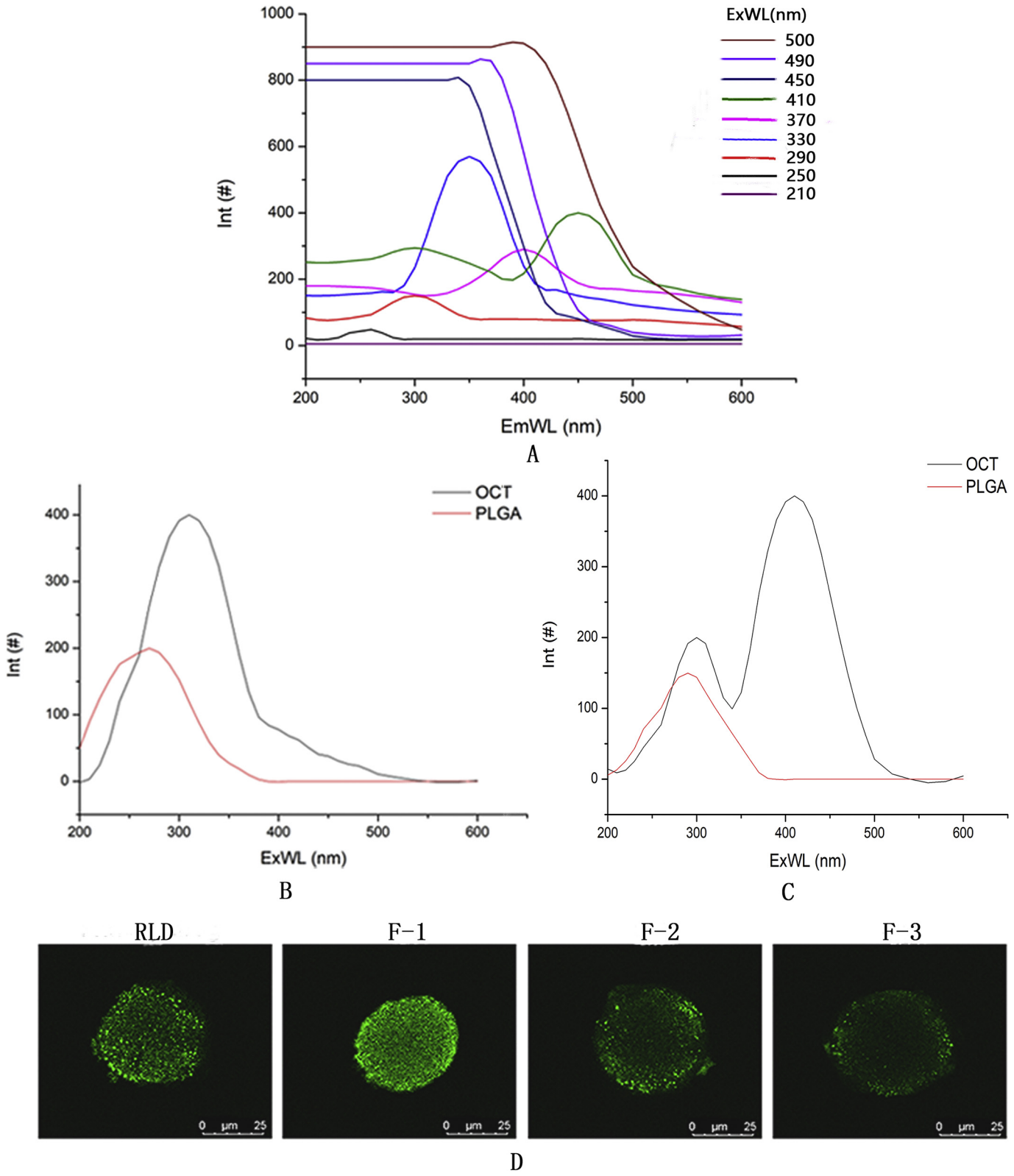

Fig. 2. Emission wavelength and fluorescence intensity of octreotide solution at different excitation wavelengths (A) (Excitation: start 190 nm, end 500 nm, step 40 nm; Emission: start 200 nm, end 600 nm, speed 1200 nm/min); A plot of the excitation wavelength versus fluorescence intensity of a drug (OCT) and a polymer (PLGA) at a certain emission wavelength (B: Emission:350 nm; C: Emission:460 nm); Fluorescence image of drug distribution on the surface of microspheres (D). Scale bar: 25 μm.

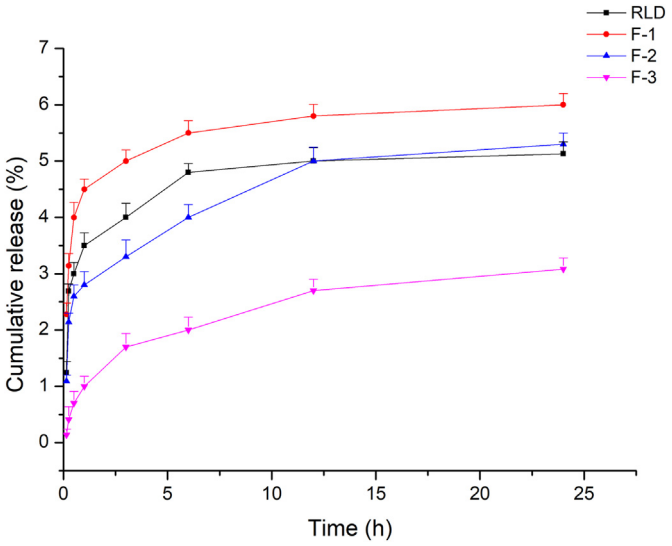

Fig. 3. Accelerated in vitro cumulative release of microspheres within 24 h (mean ± SD, $n = 6$).

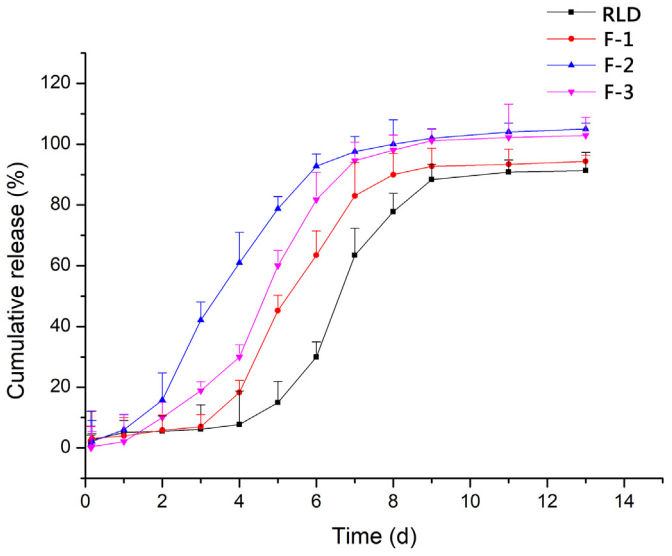

Fig. 4. Accelerated in vitro cumulative release of microspheres (mean ± SD, n = 6).

reason why Fig. 1-a differed from Fig. 1-c may be that octreotide acetate and polymer were not simply mixed or adsorbed, but in the amorphous phase, the drug was diffused in the polymer matrix to take shape a new phase (Zhu et al., 2018). This difference again proves that octreotide acetate MS has formed.

3.3. The surface distribution of the drug

At an emission wavelength of 350 nm or 460 nm, the octreotide acetate solution has a desirable fluorescence intensity (Fig. 2A). Then, it is further obtained that the excitation wavelength of the octreotide acetate solution may be 310 nm or 410 nm (Fig. 2B and C). However, the fluorescence intensity of PLGA at an emission wavelength of 350 nm (fixed excitation wavelength is 310 nm) has a certain influence on the measurement of octreotide acetate (Fig. 2B). Excitingly, PLGA does not have fluorescence intensity at the emission wavelength of 460 nm (fixed excitation wavelength is 410 nm) (Fig. 2C). Thence, the latter can be used as a condition for measuring the surface distribution of a drug.

According to the fluorescence distribution and its intensity, the distribution of the drug on the surface of the MS could be observed, and then the release of the drug was preliminarily estimated(Fig. 2D). Compared with the RLD, F-1 had a uniform fluorescence distribution and a strong signal. It could be presumed that there were more drugs on the surface and the burst release was more obvious. The fluorescence intensity of F-2 and F-3 was significantly weaker than that of the first two groups, with F-3 being the weakest. In addition, the two sets of fluorescence signals were mainly distributed at the edges and showed negligible fluorescent staining inside the matrix.

3.4. Accelerated in vitro drug release

According to the investigation, it is very cumbersome and time-consuming to obtain the in vitro release curve of the MS using a conventional "real-time" release method. Therefore, it is necessary to adopt a method of accelerating in vitro release under the premise of achieving quality control. There was an apparent difference in the initial and cumulative release of MS of the four formulations (Fig. 3 and Fig. 4). Among them, the burst release of F-1 MS was the most obvious, and the cumulative release at 1 h reached 4.5%. Both F-1 and RLD had a 4-day plateau phase after released to 5.8% and 5% (12 h), respectively. After the plateau phase, the release medium solution could contact more and more pores due to the accelerated degradation of the polymer and the rate of erosion (Gu and Burgess, 2015). On the 9th day, the drug release reached 92%, after which the drug was almost no longer released. Interestingly, when the polymer mixture was used as the carrier, the cumulative release of F-3 at 6 h was only half that of the RLD, and at this time, F-2 was about 1% lower than the RLD. The reduced burst release was the result of a reduction in surface drug distribution and subsequent drug diffusion retention, which was consistent with the fluorescence results. F-2 and F-3 remained a stable release behavior after 12 h and the drug cumulative reached 100% on the 9th day. In contrast, F-2 showed a quicker degradation than F-3 because the prioritized degradation of the higher hydrophilicity-specified ratio of glycolic acid determines that the degradation rate of PLGA 50:50 (PLA/PGA) was much quicker compared to PLGA 75:25.

3.5. Degradation image of microspheres

The morphology of the surface and cross-section of the MS was investigated by SEM (Figs. 5,6). The results showed that the MS of the four formulations were rounded, and the surface of the RLD and its interior had uniform pores which were the main cause of the sudden release. F-1 MS had evident tunnels and some large holes on the surface, and it looked like a honeycomb because it had countless pores. The surface of the F-2 MS had some holes, and the internal holes were connected to each other to form a channel leading to the surface. F-3 MS had a compact and smooth surface and internal structure. Holes generated when residual organic solvent and water were got rid of from the polymer during the drying of the MS are difficult to retract (Q. Xi et al., 2018). The reason why the surface morphology of F-2 and F-3 differs from F-1 may be that the Mw is directly related to the size of the polymer chain, and the polymer having a lower Mw has a shorter polymer chain (Kapoor et al., 2015). The interpretations from various experiments have indicated that although PLGA is hydrophobic, it still softens in the aqueous phase. This change results in a decrease in the mechanical properties of the polymer (Wu et al., 2006). Therefore, during the solidification of the microspheres with the polymer mixture as a carrier, the low Mw PLGA may cover the larger pores generated by evaporation of the solvent.

After one day of incubation, the surface of the MS of the RLD, F-1, and F-2 showed obvious ripples and small holes, of which F-1 MS were most obvious. At this time, only a small ripple appeared on the surface of the F-3 MS, but two types of pores were formed inside the F-2 and F-3 MS (as defined by IUPAC (H. Chen et al., 2014)): small pores formed near the periphery (~100 nm) and large pores (~1 μm) formed at the

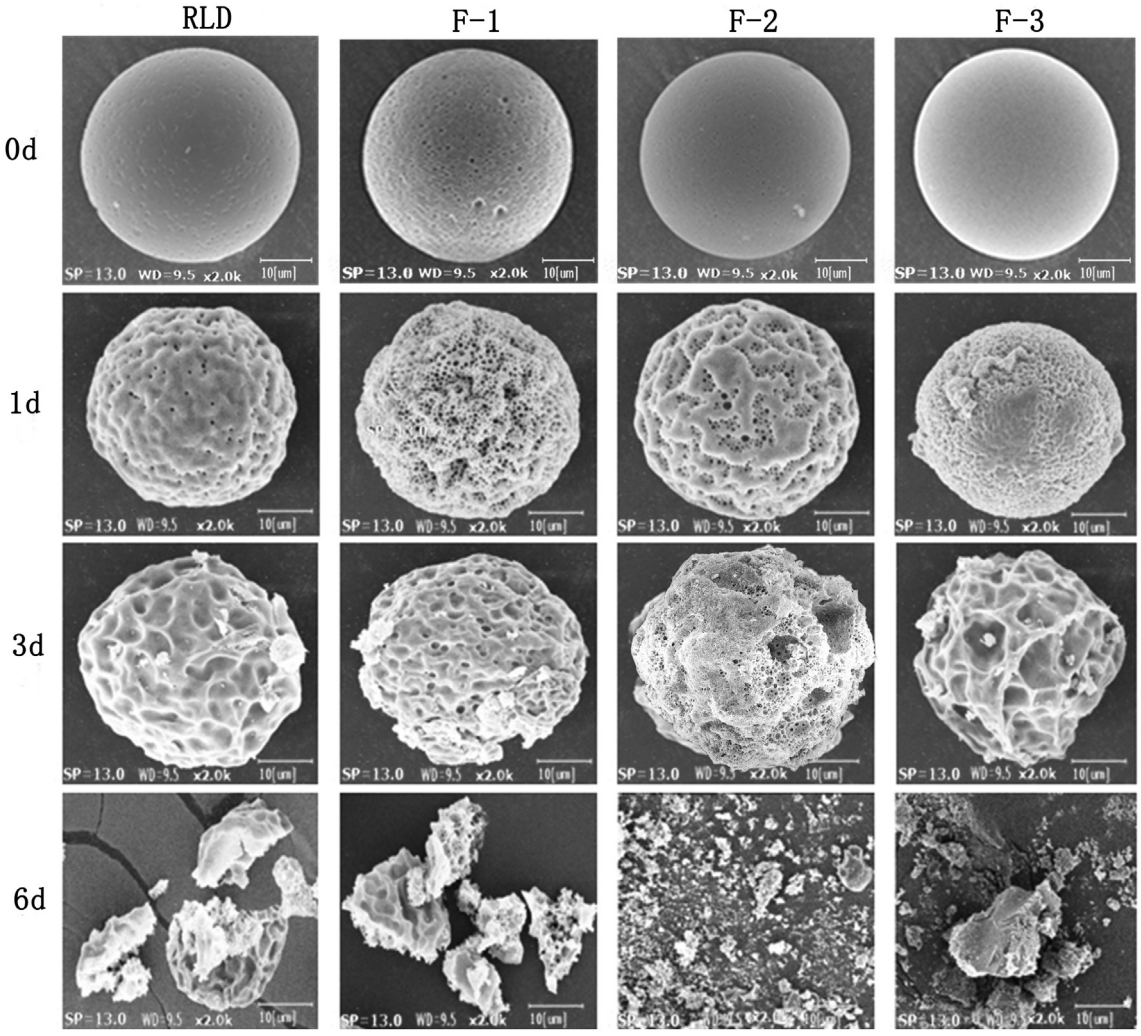

Fig. 5. SEM of the surface of the microspheres after incubation for a period of time in 5% methanolic water. Scale = 10 μm, ×2.0 k, SP = 13.0, WD = 9.5.

core center of the particles. The signs of ripples on the surface of the MS gradually progressed to day 3, when particles presented inward folding. And due to the erosion of the polymer, the surface of F-2 MS and F-3 MS even appeared concave. On day 3, the cross-sectional view of the MS showed an increase in peripheral porosity and core pore size. This phenomenon was more pronounced in F-2 and F-3. It has been reported in the literature that pore formation is generally attributed to the autocatalytic process resulting from the formation of acidic conditions in the particles due to hydrolysis of the polymer (Fan et al., 2018). On the 6th day, the polymer skeleton structure disappeared and dissolved.

3.6. Pharmacokinetic results

Fig. 7 is a graph showing the mean serum concentration of octreotide acetate versus time after a single intramuscular injection of the MS preparation per rat. The pharmacokinetic parameters are shown in Table 2. The Cmax of F-2 (Cmax = 8.4 μg/l) and F-3 (Cmax = 7.9 μg/l) were smaller than the RLD (Cmax = 14.3 μg/l), and Tmax was 15 min later than the RLD. The plasma concentration of the RLD is < 1.5 μg/l from day 3 to day 7. The peak of F-1 plasma concentration appeared on day 10 (3.4 μg/l) and day 25 (6 μg/l) after initial release, respectively, and the release trend was basically consistent with the RLD. Excitingly, the plasma concentrations in the initial stage after F-2 and F-3 administration were lower than the RLD, moreover, they remained released from day 2 to day 7 to maintain a high plasma concentration level (≥ 2 μg/l). Furthermore, the $AUC_{0-\infty}$ of both F-2 and F-3 were greater than RLD, indicating better bioavailability for both formulations.

4. Discussion

To better understand the effect of PLGA blends on drug release in MS. We compared the RLD (Sandostatin Lar) and tried to gain new insights on the mechanisms of drug release by studying changes in pores inside the MS.

In all formulations, there was a large difference in the drug loading of the MS. Compared to PGA, the methyl side chain present in PLA makes it hydrophobic (Zhou et al., 2017). As a result, as the lactide ratio increases, the hydrophilicity of PLGA gradually decreases. This increased hydrophobicity results in a faster solidify of the polymer, and as a result, the drug encapsulation can be enhanced. PLGA copolymers can cleave their skeleton ester bonds into oligomers and final monomers by hydrolysis or biodegradation. This has been indicated in vivo and in vitro for sundry drug genre and proteins/peptides with distinct polymers (Ding and Zhu, 2018). Uniform degradation of the matrix body is the primary degradation process of these polymers, where the degradation rate of the polymer is less than the rate at which water penetrates into the matrix (Bhatnagar et al., 2018). Interestingly, our data showed that when mixed polymers were used, the number and size of pores during degradation became an important factor in drug release.

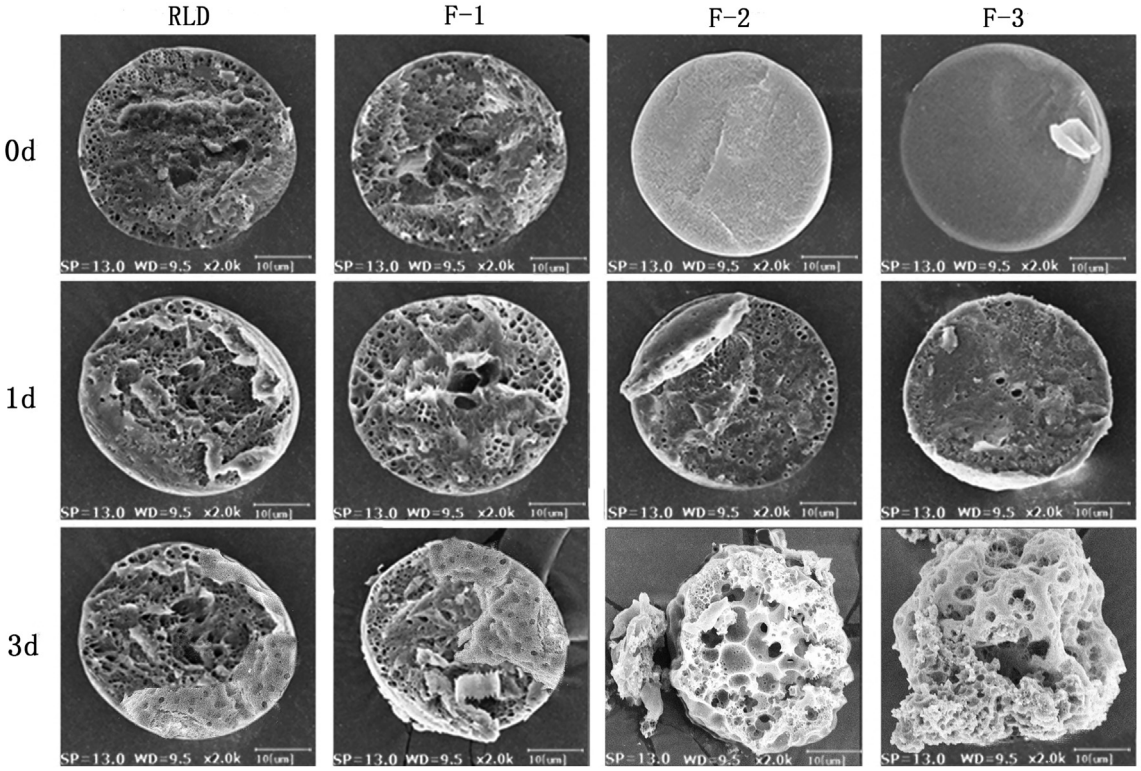

Fig. 6. SEM of the cross-section of the microspheres after incubation for a period of time in 5% methanolic water. Scale = 10 μm, ×2.0 k, SP = 13.0, WD = 9.5.

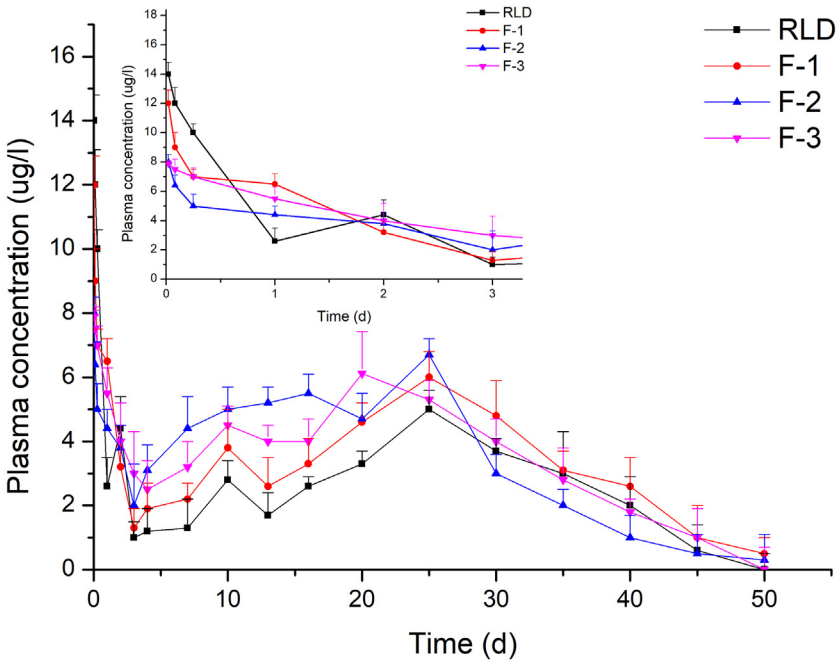

Fig. 7. Octreotide plasma concentration-time curve after intramuscular injection of different microspheres (mean ± SD, $n = 5$).

4.1. In phase I- burst release phase

With the addition of low Mw PLGA, the burst release in the first 12 h was significantly inhibited. It was not difficult to find that the initial drug release of F-2 and F-3 was much lower than that of the RLD and F-1. According to reports in the literature, the release of surface drugs and the diffusion of drugs are the main causes of the burst release (Jingcao et al., 2018). It was surmised that the existence of low Mw PLGA reduced the rate of polymer precipitation during MS solidification and extended the continuous time of the semi-solid before the glass state (Ma et al., 2018). Therefore, the polymer chains had more time to rearrange into lower energy states, as a result, the MS had a higher density and less drug diffusion. This was also evidenced by the difference in the fluorescence phenomenon of the surface drug distribution (Fig. 2) and the surface pores of the MS (Fig. 5). Furthermore, the random fragmentation of PLGA significantly reduced the Mw of the polymer, but there is no soluble monomer product formed and no significant weight loss in this stage (Hazekawa et al., 2017).

Table 2
Pharmacokinetic Parameters (mean ± SD, n = 5).

Parameters	Unit	RLD	F-1	F-2	F-3
AUC_{0-t}	μg/l * h	3358.3 ± 384.7	3763.6 ± 464.7	5007.1 ± 431.4	4821.7 ± 422.9
$AUC_{0-\infty}$	μg/l * h	3406.8 ± 384.4	4066.5 ± 327.1	5247.2 ± 405.2	5005.4 ± 786.8
Cmax	μg/l	14.3	12.1	8.4	7.9
Tmax	h	0.25	0.50	0.50	0.50
$T_{1/2}$	h	85.1 ± 17.7	98.1 ± 63.3	162.7 ± 58.8	159.8 ± 53.1
$MRT_{0-\infty}$	h	577.7 ± 110.3	564.5 ± 119.7	465.1 ± 106.8	520.8 ± 117.4

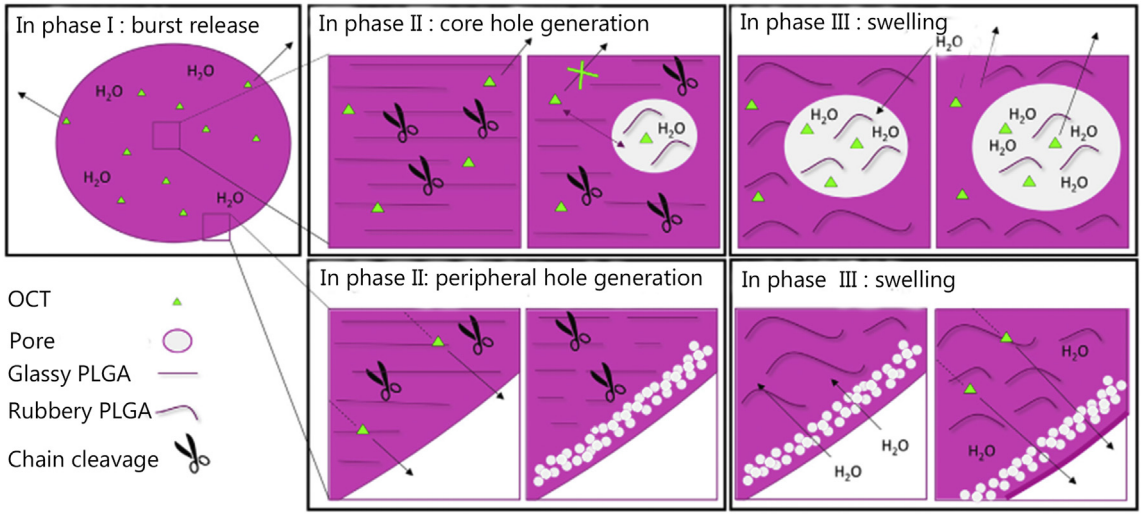

Fig. 8. The mechanism of change in the internal pores of microspheres during drug release in the formulations of F-2 and F-3.

4.2. In phase II–effect of pores on the plateau phase

In phase II, the plateau phase of the RLD and F-1 is due to the fact that the high Mw polymer chain is highly entangled and effectively prevents a large amount of particle swelling. When MS was manufactured using polymer blends, the reason why the addition of low Mw PLGA could eliminate the plateau phase can be illustrated as follows: 1) larger amounts of low Mw PLGA result in higher hydrophilicity of the MS, the more permeable water causes the polymer to crack and begin to produce peripheral and core pores. These holes are interconnected to constitute a channel to the outer surface (Han et al., 2016a, b). In addition, the presence of the core holes and the peripheral holes means that autocatalysis of PLGA occurs at the center of the particles and around the particles (Gu and Burgess, 2015). 2) due to the degradation of low Mw PLGA, the accumulation of acidic oligomers leads to an increase in local acidity, which further accelerates the erosion of the MS.

In this study, the pore size of the peripheral pores was significantly smaller than that of the core pores (Fig. 6). This may be because the peripheral pores are located close to the edge of the matrix, the acidic by-products will be quickly removed by diffusion, and the concentration may be lower than the concentration in the core pores, thus limiting the growth of the peripheral pores to some extent.

In summary, we present new evidence that the addition of low Mw PLGA results in pore changes in the MS, which may have a significant impact on the shape of the second phase of the three-phase release profile.

4.3. In phase III–swelling and pores

The drug release in phase III is almost independent of the Mw of PLGA. Because the drugs in the four formulations could be released quickly at this stage (Fig. 4). In this study, we believe that pore size and number are key parameters in determining the degree of swelling. On the third day, the size of the MS core holes not only became larger but also increased in number (Fig. 6). As described by Gu et al. (Gu et al., 2016), The polyester chain breaks under hydrolysis to weaken the entanglement of the macromolecules and cause the microparticles to swell, as a result, the volume of the polymer would also increase to some extent. In addition, the presence of degradation products increases the osmotic pressure of the system, more and more water is attracted to the particles (Gasmi et al., 2015). Therefore, the accelerated release of octreotide acetate is caused by an increase in the fluidity of the drug molecule.

4.4. Release mechanism

Based on the experimental results, Fig. 8 summarizes the mechanism of change in the internal pores of MS during drug release in the formulations of F-2 and F-3. The release of octreotide acetate is mainly from the surface of the MS in phase I. Polymer cleavage initiates the production of core and peripheral pores in phase II. These interconnected channels act as channels for the drug to pass into the release medium. In phase III, when the Mw falls below 20 kDa, the glass transition temperature of the PLGA drops obviously, causing the MS to swell (Siepmann et al., 2002). The osmotic pressure produced by swelling promotes the release of octreotide acetate.

Overall, the in vivo release profile of octreotide acetate in the RLD presented three phases, initial burst release phase due to the diffusion of the drug in the pore or channel near the surface, followed by a plateau phase of about 5 d, finally a continuous release of the peptide embedded in the polymer matrix. In contrast, the release curves of F-2 and F-3 in vivo exhibited two phases, ie, the plateau phase was eliminated, and this different absorption pattern may be attributed to the lower Mw PLGA added in the formulation. Although the difference in absorption patterns between the two formulations was small, the addition of different types of low Mw had a certain effect on drug release in vivo, and the serum levels of the drugs were comparable from day 2

to day 50. Firstly, from day 2 to day 25, the plasma concentration of F-2 was 0.8 μg/l/d higher than F-3. After 25 days, the release rate of F-2 was significantly faster than that of F-3, which was consistent with the results in vitro. These differences are due to the different ratios of lactide and glycollide.

Since octreotide acetate is effective in inhibiting hormone secretion, the use of octreotide acetate in clinical diseases associated with excessive hormone secretion such as acromegaly has been proposed (Kang et al., 2019). Therefore, the body weight of normal people decreased after the use of octreotide acetate, and in this study, the rats were also found to have a body weight loss of about 10% after 20 days of administration. Based on these results, it is expected that the pharmacological action of the octreotide acetate is maintained during drug release.

5. Conclusion

This study shows that it is highly promising to use a PLGA mixture as a carrier for delivery peptides and protein drugs to prepare a sustained release dosage form with the desired release. Compared to MS obtained using only high Mw PLGA, not only reduced burst release but also eliminated hysteresis, resulting in stable and sustained drug release behavior. This is expected to provide an optimized alternative for the treatment of acromegaly and functional tumors.

Declaration of Competing Interest

The manuscript has been reviewed and approved by all authors. There are no conflicts of interest here.

Acknowledgement

This study was supported by the Yantai University School of Pharmacy and Shandong Luye Pharmaceutical Co., Ltd.

References

Aziz, N.M., Ragy, M.M., Ahmed, S.M., 2018. Somatostatin analogue, octreotide, improves restraint stress-induced liver injury by ameliorating oxidative stress, inflammatory response, and activation of hepatic stellate cells. Cell Stress Chaperones 23 (6), 1237–1245. https://doi.org/10.1007/s12192-018-0929-7.

Bhatnagar, P., Kumari, M., Pahuja, R., Pant, A.B., Shukla, Y., Kumar, P., Gupta, K.C., 2018. Hyaluronic acid-grafted PLGA nanoparticles for the sustained delivery of berberine chloride for an efficient suppression of Ehrlich ascites tumors. Drug Deliv Transl Res 8 (3), 565–579. https://doi.org/10.1007/s13346-018-0485-9.

Casnici, C., Lattuada, D., Crotta, K., Truzzi, M.C., Corradini, C., Ingegnoli, F., ... Marelli, O., 2018. Anti-inflammatory effect of somatostatin analogue octreotide on rheumatoid arthritis synoviocytes. Inflammation 41 (5), 1648–1660. https://doi.org/10.1007/s10753-018-0808-5.

Chen, H., Zuo, D., Zhang, J., Zhou, M., Ma, L., 2014. Classification of 2-pore domain potassium channels based on rectification under quasi-physiological ionic conditions. Channels (Austin) 8 (6), 503–508. https://doi.org/10.4161/19336950.2014.973779.

Chingle, R., Proulx, C., Lubell, W.D., 2017. Azapeptide synthesis methods for expanding side-chain diversity for biomedical applications. Acc. Chem. Res. 50 (7), 1541–1556. https://doi.org/10.1021/acs.accounts.7b00114.

Ding, D., Zhu, Q., 2018. Recent advances of PLGA micro/nanoparticles for the delivery of biomacromolecular therapeutics. Mater. Sci. Eng. C Mater. Biol. Appl. 92, 1041–1060. https://doi.org/10.1016/j.msec.2017.12.036.

Fan, S., Zheng, Y., Liu, X., Fang, W., Chen, X., Liao, W., ... Liu, J., 2018. Curcumin-loaded PLGA-PEG nanoparticles conjugated with B6 peptide for potential use in Alzheimer's disease. Drug Deliv 25 (1), 1091–1102. https://doi.org/10.1080/10717544.2018.1461955.

Fredenberg S, Wahlgren M, Reslow M, et al. J. (2011). The mechanisms of drug release in poly(lactic-co-glycolic acid)-based drug delivery systems—a review. Int. J. Pharm., 415(1–2):34–52. doi:https://doi.org/10.1016/j.ijpharm.2011.05.049.

Gasmi, J.-F. Willart, Danede, F., et al., 2015. Importance of PLGA microparticle swelling for the control of prilocaine release. Journal of Drug Delivery Science and Technology 30, 123–132. https://doi.org/10.1016/j.jddst.2015.10.009.

Gu, B., Burgess, D.J., 2015. Prediction of dexamethasone release from PLGA microspheres prepared with polymer blends using a design of experiment approach. Int. J. Pharm. 495 (1), 393–403. https://doi.org/10.1016/j.ijpharm.2015.08.089.

Gu, B., Sun, X., Papadimitrakopoulos, F., Burgess, D.J., 2016. Seeing is believing, PLGA microsphere degradation revealed in PLGA microsphere/PVA hydrogel composites. J. Control. Release 228, 170–178. https://doi.org/10.1016/j.jconrel.2016.03.011.

Han, F.Y., Thurecht, K.J., Whittaker, A.K., Smith, M.T., 2016a. Bioerodable PLGA-based microparticles for producing sustained-release drug formulations and strategies for improving drug loading. Front. Pharmacol. 7, 185. https://doi.org/10.3389/fphar.2016.00185.

Han, S., Zhang, X., Li, M., 2016b. Progress in research and application of PLGA embolic microspheres. Front Biosci (Landmark Ed) 21, 931–940.

Hazekawa, M., Kojima, H., Haraguchi, T., Yoshida, M., Uchida, T., 2017. Effect of self-healing encapsulation on the initial burst Release from PLGA microspheres containing a long-acting prostacyclin agonist, ONO-1301. Chem Pharm Bull (Tokyo) 65 (7), 653–659. https://doi.org/10.1248/cpb.c17-00025.

Hu, Z., Liu, Y., Yuan, W., Wu, F., Su, J., Jin, T., 2011. Effect of bases with different solubility on the release behavior of risperidone loaded PLGA microspheres. Colloids Surf B Biointerfaces 86 (1), 206–211. https://doi.org/10.1016/j.colsurfb.2011.03.043.

Huang, X., Li, N., Wang, D., Luo, Y., Wu, Z., Guo, Z., Wu, C., 2015. Quantitative three-dimensional analysis of poly (lactic-co-glycolic acid) microsphere using hard X-ray nano-tomography revealed correlation between structural parameters and drug burst release. J. Pharm. Biomed. Anal. 112, 43–49. https://doi.org/10.1016/j.jpba.2015.04.017.

Jingcao, L., Lan, S., Yan, L., et al., 2018. To reduce premature drug release while ensure burst intracellular drug release of solid lipid nanoparticle-based drug delivery system with clathrin modification. Nanomedicine. https://doi.org/10.1016/j.nano.2018.05.014.

Kang, S., Yoon, J.S., Lee, J.Y., Kim, H.J., Park, K., Kim, S.E., 2019. Long-term local PDGF delivery using porous microspheres modified with heparin for tendon healing of rotator cuff tendinitis in a rabbit model. Carbohydr. Polym. 209, 372–381. https://doi.org/10.1016/j.carbpol.2019.01.017.

Kapoor, D.N., Bhatia, A., Kaur, R., et al., 2015. PLGA: a unique polymer for drug delivery [J]. Ther. Deliv. 6 (1), 41–58.

Liu, C., Lu, Q., Qu, H., Geng, L., Bian, M., Huang, M., ... Zhang, Z., 2017. Different dosages of mifepristone versus enantone to treat uterine fibroids: a multicenter randomized controlled trial. Medicine (Baltimore) 96 (7), e6124. https://doi.org/10.1097/MD.0000000000006124.

Ma, C.H., Zhang, H.B., Yang, S.M., Yin, R.X., Yao, X.J., Zhang, W.J., 2018. Comparison of the degradation behavior of PLGA scaffolds in micro-channel, shaking, and static conditions. Biomicrofluidics 12 (3), 034106. https://doi.org/10.1063/1.5021394.

Ohlmann, C.H., Gross-Langenhoff, M., 2018. Efficacy and tolerability of leuprorelin acetate (Eligard (R)) in daily practice in Germany: pooled data from 2 prospective, non-interventional studies with 3- or 6-month depot formulations in patients with advanced prostate cancer. Urol. Int. 100 (1), 66–71. https://doi.org/10.1159/000479187.

Orlewska, E., Stepien, R., Orlewska, K., 2018. Cost-effectiveness of somatostatin analogues in the treatment of acromegaly. Expert Rev Pharmacoecon Outcomes Res 1–11. https://doi.org/10.1080/14737167.2018.1513330.

Siepmann, J., Faisant, N., Benoit, J.P., 2002. A new mathematical model quantifying drug release from bioerodible microparticles using Monte Carlo simulations[J]. Pharmaceutical Research (Dordrecht) 19 (12), 1885–1893. https://doi.org/10.1023/a:1021457911533.

Sun, H., Zou, S., Candiotti, K.A., Peng, Y., Zhang, Q., Xiao, W., ... Yang, J., 2017. Octreotide attenuates acute kidney injury after hepatic ischemia and reperfusion by enhancing autophagy. Sci. Rep. 7, 42701. https://doi.org/10.1038/srep42701.

Tiberg, F., Roberts, J., Cervin, C., Johnsson, M., Sarp, S., Tripathi, A.P., Linden, M., 2015. Octreotide s.c. depot provides sustained octreotide bioavailability and similar IGF-1 suppression to octreotide LAR in healthy volunteers. Br. J. Clin. Pharmacol. 80 (3), 460–472. https://doi.org/10.1111/bcp.12698.

Wang, Y., Gu, B., Burgess, D.J., 2014. Microspheres prepared with PLGA blends for delivery of dexamethasone for implantable medical devices[J]. Pharm. Res. 31 (2), 373–381.

Wu, L., Zhang, J., Jing, D., Ding, J., 2006. Wet state mechanical properties of three dimensional polyester porous scaffolds. J. Biomed. Mater. Res. A 76, 264–271.

Xi, Q., Ping, R., Liu, X., et al., 2018. Synthesis of hollow polysaccharide microspheres with hierarchically porous structure in alkali/urea mixture through freeze-drying[J]. Mater. Lett. 228, 229–231.

Zhou, F.L., Chirazi, A., Gough, J.E., Hubbard Cristinacce, P.L., Parker, G.J.M., 2017. Hollow polycaprolactone microspheres with/without a single surface hole by co-electrospraying. Langmuir 33 (46), 13262–13271. https://doi.org/10.1021/acs.langmuir.7b01985.

Zhu, S., Dou, M., Huang, G., 2018. Intratumoral Injection Administration of Irinotecan-Loaded Microspheres: in vitro and in vivo evaluation[J]. AAPS PharmSciTech 19 (8), 3829–3838. https://doi.org/10.1208/s12249-018-1167-0.